Journal of Sustainability Science and Management
Volume 17 Number 12, December 2022: 24-39
eISSN: 2672-7226

DEVELOPMENT OF AGRO-BASED NANOFILTERS TO CAPTURE SUSPENDED TITANIUM IN AIR

SHAHRULNIZAM JAMEN[1,4]*, ZAKUAN AZIZI SHAMSUL HARUMAIN[2], MARYAM ZAHABA[3], WAN HAZMAN DANIAL[3], MOHD SHUKRI MOHD ARIS[4], SITI NURNAFISAH MOHD ZURAIDI[2], MOHD SYAHMI IDRIS[2], WAN LUTFIL HADI WAN ZAIN[3] AND HAZRIN ABDUL HADI[5]

[1]National Institute of Occupational Safety and Health, 43650 Bandar Baru Bangi, Selangor, Malaysia. [2]Department of Biotechnology, Kulliyyah of Science, International Islamic University Malaysia, Bandar Indera Mahkota Campus, 25200 Kuantan, Pahang, Malaysia. [3]Department of Chemistry, Kulliyyah of Science, International Islamic University Malaysia, Bandar Indera Mahkota Campus, 25200 Kuantan, Pahang, Malaysia. [4]Occupational Health and Safety Risk Management (OHSeRM) Research Initiative Group & Centre for Environmental Health & Safety, Universiti Teknologi MARA, Faculty of Health Sciences, Puncak Alam Campus, 42300 Bandar Puncak Alam, Selangor, Malaysia. [5]IIUM Entrepreneurship and Consultancies Sdn. Bhd., Research Management Centre, International Islamic University Malaysia, Jalan Gombak, 53100 Kuala Lumpur, Malaysia.

**Corresponding author: shahrulnizam.jamen@niosh.com.my*
Submitted final draft: 27 May 2022 *Accepted: 20 June 2022* http://doi.org/10.46754/jssm.2022.12.004

Abstract: Nanosilica and nanozeolite synthesised from rice husk (RH) were investigated for their potential to develop a low-cost nanofilter membrane as an alternative to replace nylon membrane used in the Nanoparticle Respiratory Deposition (NRD) sampler for capturing titanium dioxide (TiO_2) nanoparticles suspended in the air. Due to its exceptional adsorption capacity to many inorganic materials, graphene oxide was also investigated for its potential to capture the TiO_2 nanoparticles to compare its performance with the newly developed agro-based nanofilters. All nanofillers were developed by depositing the synthesised nanomaterials on a polyvinylidene fluoride (PVDF) membrane using the layer deposition method and characterised by Field Emission Scanning Microscopy/Energy Dispersive X-ray (FESEM-EDX) analysis. Each nanofilters developed were exposed to TiO_2 nanoparticles for 15 minutes with an average airflow of 2.5 L/minutes and were compared with the conventional nylon membrane used in NRD. Among all nanofilters developed, nanozeolite filter (0.1% w/v) showed the highest concentration of Ti captured (81.7 µg/g) compared to nanosilica (56.7 µg/g) and graphene oxide (8.2 µg/g) filters. Interestingly, all developed nanofilters did not show any presence of Ti in their background levels, further suggesting its purity in capturing Ti nanoparticles in the air.

Keywords: Nanosilica, nanozeolite, graphene, titanium, nanofilter.

Introduction

Nanomaterials are materials with an external dimension of 1-100 nm (Jeevanandam *et al*., 2018). Recent advancements in nanotechnology have gained much interest in applying nanomaterials as catalysts, sensors and adsorbents due to their high reactivity and greater specific surface area (Khan *et al*., 2019). Nanomaterials, however, might also bring about fresh dangers and particular uncertainty in matters of occupational safety and health (OSH). The most recent and concerning problem involves the increased use and manufacture of TiO_2 nanoparticles and their effects on the workforce.

TiO_2 is a naturally occurring mineral existing in a few crystalline. TiO_2 is a white in colour, odourless, tasteless chemical and can be produced from mined ilmenite ore through the sulphate or chloride process. Due to its ability to be resistant to chemical attack and possess excellent thermal stability (Vaquero *et al*., 2016), TiO_2 is also widely used in many commercial products including paints (Fichera *et al*., 2019), cosmetics (Dréno *et al*., 2019), food (Musial *et al*., 2020), aerospace (Inagaki *et al*., 2014) and many more.

Despite its tremendous usage, TiO_2 nanoparticles may also possess greater health risks for workers in the titanium-based industry

due to their carcinogenic effect (*Titanium Dioxide: OSH Answers*, 2017). TiO_2 main route of exposure to the human body is through skin contact and inhalation (Skocaj *et al*., 2011). Inhalation at high concentrations can cause severe health effects because it is classified under "respirable" particles; when inhaled, they are capable of being deposited in the gas-exchange (alveolar) region of the lungs (Ursini *et al*., 2014; Horváth *et al*., 2019; Papp *et al*., 2020).

NRD personal samplers are used for occupational safety and health monitoring to assess the exposure of workers to respirable titanium nanoparticles. NRD is a device that collects respirable particulates and nanoparticles in the air (Park *et al*., 2015). NRD is light in weight (~60 g) and thus, can be attached to the workers and easily be carried throughout the working hour (Cena *et al*., 2011). It consists of three main parts: Cyclone, impaction and diffusion (Koehler & Peters, 2015). Particles smaller than 300 nm will be able to pass through to the diffusion stage to be collected by the final filter made of nylon. However, Mines *et al*. (2016) indicated that the nylon mesh filter contains a substantial amount of titanium, most likely used in whitening the nylon materials. This may interfere with the purity and efficiency of the NRD assessment towards TiO_2 exposure. The large pore size of the nylon filter (11 µm) might also contribute to its inefficiency as larger particles are presumed to be deposited on the filter instead of the targeted titanium nanoparticles (Mines *et al*., 2016). Thus, a much more specific nanofilter is required to increase the efficiency in monitoring the exposure of titanium nanoparticles towards workers.

In this work, we investigated the potential of nanosilica and nanozeolite synthesised from rice husk (RH) and graphene oxide as the main material in developing a low-cost nanofilter membrane as an alternative to replacing the nylon membrane used in the NRD sampler.

Materials and Methods

Synthesis of Nanosilica

The extraction of nanosilica from RH began with the pre-treatment of RH by acid leaching using hydrochloric acid (HCl) to remove metallic impurities and enhance the nanosilica purity (Ruey *et al*., 2020). RH was washed thoroughly with distilled water to remove contaminants and dried in an oven at 110°C for 24 hours. Next, 40 g of dried RH was mixed with 1,000 mL of 1N HCl at 80°C while stirring for 2 hours (Patil *et al*., 2014). The RH was then filtered and rinsed several times with distilled water until it reached pH 7. White RHA was produced after the thermal treatment using a furnace for 6 hours at a temperature of 700°C to remove inorganic impurities through a decomposition process. 5 g of white RHA was then mixed with 150 mL of 2.5N NaOH while stirring at 80°C for 1.5 hours. The mixture was then filtered to obtain a viscous and colourless sodium silicate (Na_2SiO_3) solution. Next, concentrated sulfuric acid (H_2SO_4) was slowly added into the Na_2SiO_3 solution while stirring at pH 2 (Yuvakkumar *et al*., 2014) until silica precipitate was formed. The resulting precipitate was rinsed 3 times using a centrifuge at 4,000 rpm for 3 minutes and burned at 800°C for 3 hours in a furnace, then, crushing the dried nanosilica using stone mortar to obtain various sizes of nanosilica powder.

Synthesis of Nanozeolite

The process of nanozeolite synthesis was initiated by mixing two different nanozeolite initiator solutions to obtain a gel mixture based on the work done by Ng *et al.* (2015). The first solution, silica starter was prepared by dissolving 3 g of RH with 13 g NaOH in 17 mL distilled water while stirring vigorously at 90°C for 2 hours. The second solution of the alumina initiator was prepared by dissolving 1.9 g sodium aluminate ($NaAlO_2$) powder with 0.5 g NaOH in 23 mL distilled water. The alumina

solution was slowly poured into the silica solution while stirring vigorously in a container filled with cold water for 10 minutes until a gel solution was formed. The container was then covered with aluminium foil and stored in the store below room temperature for 24 hours to produce nanozeolite crystals. The crystallisation process was interrupted several times, namely 5 minutes, 10 hours, 18 hours and 24 hours by stirring the mixture slowly to ensure consistent size and avoid sediment formation. After 24 hours, the mixture was stirred at a speed of 9,000 rpm for 60 minutes, followed by a diffusion process in distilled water. This step was repeated until the colloidal suspension reached pH 8.5. The nanozeolite extract was then dried in an oven at 110°C for 24 hours. Finally, the dried nanozeolite was crushed using a stone mortar to obtain nanozeolite powder.

Synthesis of Graphene Oxide (GO)

The preparation of GO was adapted based on an improved Hummer's method (Hou *et al*., 2020). Briefly, 3.0 g of graphite powder was mixed with 70 mL H_2SO_4 in a 500 mL beaker. The mixture was then cooled using a water bath. 9.0 g of potassium permanganate ($KMnO_4$) was slowly added to the mixture while the temperature was below 20°C. Next, the ice bath was removed and the mixture was transferred into 35°C to 40°C water bath for about half an hour. 150 mL of distilled water was then added to the mixture with continuous stirring at 95°C for 15 minutes. Another 500 mL of distilled water was added to the mixture, followed by the slow addition of 15 mL of hydrogen peroxide (H_2O_2). Afterwards, the mixture was centrifuged at 5,000 rpm for 30 minutes to remove aggregates. Then, the mixture was washed using 10% HCl twice to remove metal ion residues. During washing, the mixture was stirred thoroughly and centrifuged at 5,000 rpm for 15 minutes, followed by washing with distilled water repeatedly until it reached a constant pH. The mixture was then sonicated for 1 hour to form GO suspension and centrifuged for 5 minutes at 3,500 rpm to remove large and unexfoliated aggregates.

Characterisation of Raw Nanomaterials

The instruments used for the characterisation of the raw nanomaterials were Attenuated Total Reflection Fourier Transform Infrared Spectrometer (ATR-FTIR) (Perkin Elmer) to identify the functional groups and Transmission Electron Microscopy (TEM) (Zeiss LIBRA 120) to examine the morphology, size and distribution of the nanomaterials. FTIR measurement was performed at room temperature 400 – 4,000 cm^{-1} at Kulliyyah of Science, IIUM. Each nanosilica, nanozeolite and GO powder was mixed with potassium bromide (KBr) at the ratio of 1:100 and the mixtures were subjected to a load of 10 tons/cm^2 in an evocable die to produce clear homogeneous discs. Then, the disc obtained was measured directly to identify the functional groups and chemical bonds in a molecule in a molecule with the application of the infrared absorption spectrum. The infrared spectrum was plotted with wavenumber (cm^{-1}) against transmittance (%). TEM analysis was carried out by first preparing the sample before the analysis. Each nanomaterial was diluted in distilled water and sonicated for 15 minutes. 1 ml of the diluted sample was dropped on carbon film using a dropper. The sample was subjected to TEM analysis after drying up and non-agglomerated particles were considered.

Development of Nanofilters

A commercial PVDF membrane filter (hydrophilic) with a pore size of 0.22 µm was purchased from Bioflow Lifescience Sdn. Bhd. (Malaysia). Three different nanofilters were produced using nanosilica, nanozeolite and GO at various concentrations (0.01%, 0.05%, 0.1%, 0.5% and 1% by weight/volume). The filters were produced using a layer deposition technique assisted by vacuum filtration (Wang *et al*., 2019). The filters were produced through three stages. First, 5 mL of each nanosilica, nanozeolite or GO solution was pipetted onto a PVDF membrane filter. Then, the solution was vacuumed to produce PVDF-nanosilica, PVDF-nanozeolite or PVDF GO membrane filters. Finally, the filter was allowed to dry at room temperature. This step was repeated to

produce filters from different concentrations of nanosilica, nanozeolite and GO.

Characterisation of Nanofilters

The developed nanofilters were imaged through Field-Electron Scanning Electron Microscopy-Energy Dispersive X-Ray Spectroscopy (FESEM-EDX) (Joel, Japan) at Universiti Malaysia Pahang (UMP). Small parts of prepared filters were cut and stuck to a metal plate using carbon tape. The samples were then coated using platinum, an excellent coating material for standard FESEM applications as it can prevent charging of the sample, so the image can be captured clearer with desired magnification. The surface and composition of nylon membrane, control PVDF and nanofilters membranes were compared. This microscopic technique is a direct technique to determine the structure and morphology of the developed filter. Energy dispersive x-ray (EDX) analysis was used to identify the type of element present on the surface of the developed composite filter.

TiO_2 Nanoparticles Exposure Test

By adopting the method used in the NRD system (Cena *et al*., 2011), each nanofilters developed were exposed to TiO_2 nanoparticles. The TiO_2 nanoparticles captured in each filter were compared to the original nylon filters used in the NRD system. The setting up of the experiment was in "sealed condition" to minimise the risk of exposure to TiO_2 during the experimental process. To prepare the TiO_2 nanoparticles, 0.1 g of TiO_2 nanoparticles (Sigma Aldrich) from each 30, 50 and 100 nm were weighed, mixed and placed in a Buchner flask, followed by drying in the oven for 15 minutes to dry the mixture. The Buchner flask was then connected to the NRD set and was sealed using parafilm to prevent air leakage during the experiment. Following the original setup of the NRD system, 9 layers of nylon filters with a diameter of 25 mm were placed at the diffusion stage for each sampling cycle (Cena *et al*., 2011). However, only one layer of each newly developed nanofilters was used to replace the nylon filters using the NRD set. An air pump was connected using a rubber tube to the side arm of the Buchner flask to provide airflow for the experimental setup and the rate of the airflow was regulated to 2.5 L/minutes using a regulator connected to the NRD set. This experimental setup was aligned with existing standards by NIOSH US with a recommended exposure limit of 1.5 mg/m^3 for TiO_2 and 0.1 mg/m^3 for Ultrium TiO_2 as TWA concentrations for 10 hours per day at every 40 working hours for a week. Each filter was exposed to the suspended TiO_2 nanoparticles for 15 minutes. To avoid cross-contamination of TiO_2 nanoparticles, the NRD system was cleaned using a brush, washed and dried every time before a new filter was tested (Edu & Lai, 2015). The experiment was done in triplicate for each filter tested.

Analysis of Nanofilters Exposed to TiO_2 Nanoparticles in the Air Using ICP-MS

Before digestion, the tested filters were dried in an oven at 60°C for 2 hours to prevent decomposition or weight loss by respiration. 0.5 g of each dried filter was placed in a digestive vessel before being transferred to a high-temperature compound (HTC) safety shield. The digestive acid used in microwave acid digestion consists of 7 mL HNO_3 65% and 3 mL HCl 37% was also introduced into the digestive vessel and heated to a temperature of 110°C and 200°C for 15 minutes to ensure that the sample was dissolved so that it can be used for trace metal analysis. The sample solution was then placed in a 50 mL volumetric flask and diluted with 2% HNO_3. Each sample solution will be labelled and stored before being analysed with ICP-MS (Agilent 7500a). The exposed filters were also analysed using FESEM-EDX as described above.

Results and Discussion

Synthesis and Characterisation of Nanomaterials

Nanosilica and nanozeolite are two agricultural-based nanomaterials that can be synthesised from RH. RH are residues produced during

the rice milling process and constitute about 20% of the total paddy production (Chun & Lee, 2020). RHA contains a huge amount (85-95%) of amorphous silica (Hossain *et al*., 2018) and is identified to be the precursor for renewable nanosilica and nanozeolite in future application of advanced materials, i.e., carbon/ silica composites (Kumagai & Sasaki, 2009) and photocatalysts (Artkla *et al*., 2009). This work used chemical methods (acid washing, alkali extraction and acid precipitation) to produce a white nanosilica powder from RHA. The silica obtained was also successfully used as a precursor to react with alumina to synthesise nanozeolite powder (Figure 1). Also, in this study, an improved Hummers' method for synthesising graphene oxide was carried out without using NaNO3 in the reaction as an eco-friendly approach and produce higher reaction yield while reducing toxic gas evolution. Common Hummers' method that used $NaNO_3$ exhibits two flaws which are detected in the chemical reaction such as emission of toxic gases for instance NO_2 and N_2O_4 as well as difficult removal of Na^+ and NO_3^- ions formed during synthesising and purifying graphene oxide.

FTIR and TEM analysis was performed to identify the functional groups and sizes in all three nanomaterials produced. As observed in Figure 2 (a), the FTIR spectrum of nanosilica powder in the 400 - 4,000 cm^{-1} range shows high-intensity bands at 1,101.14, 812.84 and 467.95 cm^{-1} which were due to the asymmetric, symmetric and bending modes of SiO_2, respectively (Rafiee *et al*., 2012). The absorption peak observed at 3,442.48 cm^{-1} indicates the presence of the -OH groups due to the water molecules being chemically and physically absorbed on the nanosilica surface (Zhou *et al*., 2001; Premaratne *et al*., 2014; Pham *et al*., 2018). The subsequent peaks at 1,281 - 2,828 cm^{-1} were due to impurities such as sodium (Na) and carbonate groups (Yuvakkumar *et al*., 2014).

In Figure 2 (b), absorption at 455 cm^{-1} indicates the presence of bending vibration of the SiO_4 and AlO_4 internal tetrahedra (Ghasemi & Younesi, 2012). Absorption at 779 and 994 cm^{-1} are assigned to external symmetrical and internal asymmetrical stretching bands of T-O-T (T=Si, Al) (Ng *et al*., 2015) while the double ring vibration at 559 and 664 cm^{-1} suggests that the Na-X phase is presence (Ghasemi & Younesi, 2012). The 3,468 cm^{-1} peaks between the 3,100 - 3,600 cm^{-1} regions are due to surface hydroxyl groups such as hydrogen (H) associated with O ions on the nanozeolite lattice structure. The water deformation mode can be seen at a sharp peak of 1,646 cm^{-1} in the spectrum because zeolite sodalites generally contain NaOH and water (H_2O). TEM image resulted in a uniform nanozeolite shape in a cuboidal particle with an average diameter between 19 - 22 nm. The clumped structures could be due to a lack of

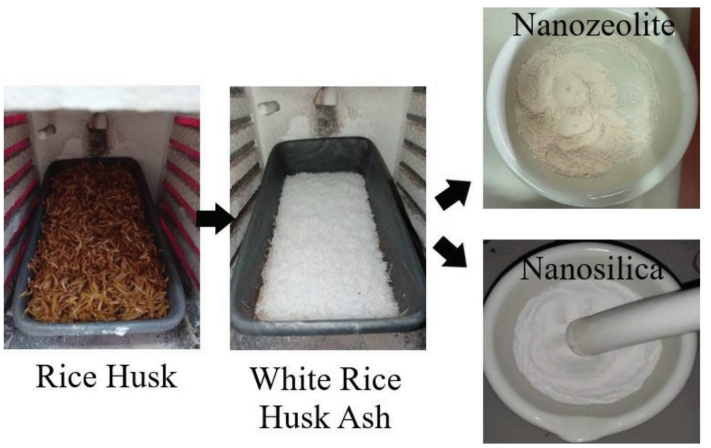

Figure 1: Synthesis of nanozeolite and nanosilica from rice husk

time in sonication while preparing the sample for analysis. The FTIR and TEM results suggest that the synthesis of nanozeolite Na-X from RHA is achieved.

Figure 2 (c) below shows that GO was successfully produced as significant peaks appeared compared to the spectrum of raw graphite powder. The spectrum of GO flakes prepared includes five more intensive peaks, as seen in the figure. The peaks belonged to the vibration of the carbon skeleton and functional groups generated during the oxidation of graphite. In particular, the GO molecules were present in carbonyl groups (C=O) and hydroxyl groups (-OH). The peak at 1,053 cm^{-1} could be referred to as the stretching vibration of the epoxide group and the bending vibration of C-H groups was also visible in the spectrum at 1,382 cm^{-1}. At 1,621cm^{-1}, a clear peak can be attributed to C=C stretching absorption and a medium absorption peak was visible at 1,728 cm^{-1} due to the carbonyl group. The O-H stretching vibration at 3,218 cm^{-1} indicated a hydroxyl group of GO and residual water between GO sheets. The TEM image indicates the presence of a thin, relatively transparent and crumpled layer of GO sheet. The wrinkled surface of the graphene oxide provides stability and prevents graphitic stacking formation (Ramos-Galicia *et al*., 2013).

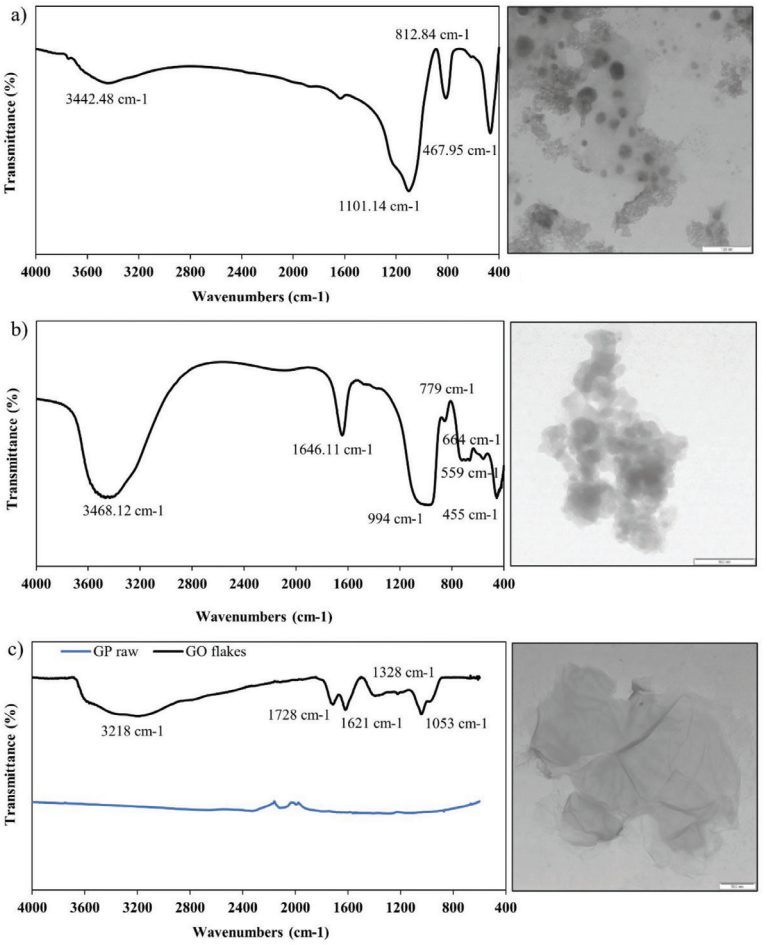

Figure 2: FTIR spectra in the range of 400 – 4,000 cm^{-1} and TEM images with the scale of 100 nm for (a) nanosilica synthesised from RHA, (b) nanozeolite synthesised from RHA and (c) graphene oxide flakes

Development and Characterisation of Nanofilters

Three different types of nanofilter membranes were developed using each nanosilica, nanozeolite and GO by depositing different concentrations of nanomaterials on polyvinylidene fluoride (PVDF) membrane facilitated by vacuum filtration (Wang *et al*., 2019) (Figure 3). In nature, the PVDF membrane is generally hydrophobic. However, this work used a modified version of the PVDF membrane with high hydrophilicity characteristics instead. Thus, this was an advantage when developing the nanofilters since all nanomaterials tested (nanosilica, nanozeolite and GO) are hydrophilic. Previous works demonstrated that modified PVDF membranes with hydrophilic surfaces possessed an improved membrane surface hydrophilicity when treated with hydrophilic materials such as silica oxide (Ruan *et al.,* 2015; Arahman *et al*., 2019) and nanozeolite (Nassrullah *et al*., 2020), thus, improving its water permeability (Arahman *et al*., 2019). Other than that, the PVDF membrane was also chosen in this work due to its ideal membrane characteristics such as having high resistance to thermal change, possessing good chemical stability (Wang *et al*., 2019) and most importantly, having much smaller pores (0.22 µm) compared to the conventional nylon filter (11 µm) used in the NRD system. It was discovered that adding nanozeolite to the PVDF membrane's surface increased the membrane's porosity without reducing its permeability (Nassrullah *et al*., 2020). Increased polarity on the surface of the hydrophilic PVDF membrane brought about by the addition of hydrophilic nanoparticles improves the propensity of inorganic nanomaterials like TiO_2 to bind to the surface as observed in recent work by Victor *et al.* (2021).

FESEM and EDX analysis was conducted to observe the PVDF membrane surface after being coated with nanosilica, nanozeolite and GO of varying concentrations (Figure 4). Figure 4 (a) illustrates the pristine PVDF membrane with intertwined fibres forming a porous network with an estimated size of pores between 0.20 to 0.60 µm. These range pore sizes of the filter may only be able to trap particles with size above ~600 nm. The pore size, however, cannot efficiently capture nanoparticles lower than 100 nm. The EDX data confirmed the presence of carbon, fluorine and oxygen compounds on the pristine PVDF membrane as observed in previous work (Scorrano *et al*., 2015) which indicates that the membrane was made of polymer consisting of carbon and fluorine.

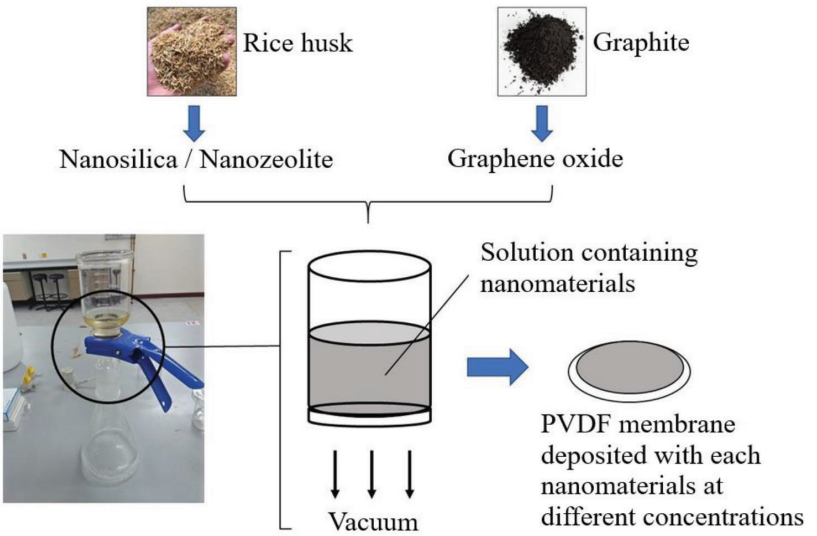

Figure 3: Schematic illustration of the preparation of nanofilter using PVDF membrane

Fair distribution of nanosilica, nanozeolite and GO nanomaterials on the PVDF membrane, as observed in the FESEM images, indicate that the vacuum filtration method managed to deposit the nanomaterials on the surface of the PVDF membrane [Figures 4 (b, c and d)]. The EDX data on the PVDF membrane with the addition of nanosilica confirmed the presence of silica (Si). As for nanozeolite, the presence of compulsory elements representing nanozeolite such as Na, Al and Si spectrum, suggests that pure nanozeolite had been deposited on the surface of the PVDF membrane as observed in the literature (Nassrullah *et al*., 2020). Based on the presence of a thin, wrinkle-like layer of graphene oxide, the FESEM picture of the GO-PVDF membranes shows that graphene oxide stacking is present on top of the porous PVDF membrane surface. According to the EDX analysis table, the high percentage of carbon and oxygen elements present denotes successful oxidation and the creation of graphene oxide. Compared to the control PVDF membrane, the fluorine weight percentage was much lower which was also caused by the increased thickness of the GO overlaying the PVDF membrane.

In this work, different concentrations of nanomaterials (0, 0.1, 0.5 and 1% w/v) added onto the PVDF membrane were analysed using FESEM-EDX. Images obtained from FESEM analysis indicate that the concentration, turbidity and thickness increased as the concentration of nanomaterials added increased (Figures 5 and 6). Similarly, it can be observed that the presence of wrinkle-like GO layering on the PVDF membrane increased with an increased amount of GO (Figure 7). The higher the GO concentration, the more crumple and wrinkle structures become more accentuated on the surface of the composite filter prepared, indicating thicker GO sheets were stacked on the surface. This was supported by the distribution of chemical weight (%) on all samples based on the EDX analysis as stated in Table 1. The weight (%) of Si increased as the concentration of nanosilica and nanozeolite on the membrane increased. The absence of fluorine in 0.5 and 1% w/v of nanosilica and nanozeolite suggest that both nanomaterials had successfully covered the surface of the membrane. The weight (%) of Si and Al increased as the contraction of nanozeolite added increased as expected due to adding more nanozeolite on the membrane. However, the weight (%) of Na did not show many changes compared to all concentrations. As for GO, the weight (%) of carbon increased starting from 0.1% to 1.0% of GO-PVDF membrane, confirming the GO concentration increased between the filters. Based on the results, it can be suggested that all nanomaterials were successfully deposited on the PVDF membrane for further experiments.

Performance of Developed Nanofilters in Capturing TiO_2 Nanoparticles in Air

The newly developed nanofilters were tested for their ability to capture TiO_2 nanoparticles by comparing them with the conventional nylon membrane used in the NRD set. Lab scale experimental setup, including the airflow was designed to represent a sampling procedure using the NRD personal sampling method described by Cena *et al*. (2011). After the nanofilters were exposed to TiO_2-containing air for 15 minutes, all filters were sent for analysis using ICP-MS to measure the total Ti concentration. In this test, five types of nanomaterial concentrations were tested 0.01%, 0.05%, 0.1%, 0.5% and 1% w/v of nanosilica, nanozeolite or GO deposited on a PVDF membrane filter. Nylon and PVDF filters without any nanomaterials were used as control.

Before analysis using ICP-MS, all filters were digested using acid to clean the sample from any impurities. In order to safely reach higher local temperatures and pressures necessary to disrupt the crucial TiO_2 lattice structure for precise measurement of titanium (Ti) counts by ICP-MS analysis, microwave digestion is considered a good option (Mines *et al*., 2016). Although microwave digestion has long been used, this is the first study conducted on the potential use of quantification in the evaluation of the exposure of TiO_2 nanoparticles on newly developed nanofilters from agricultural waste.

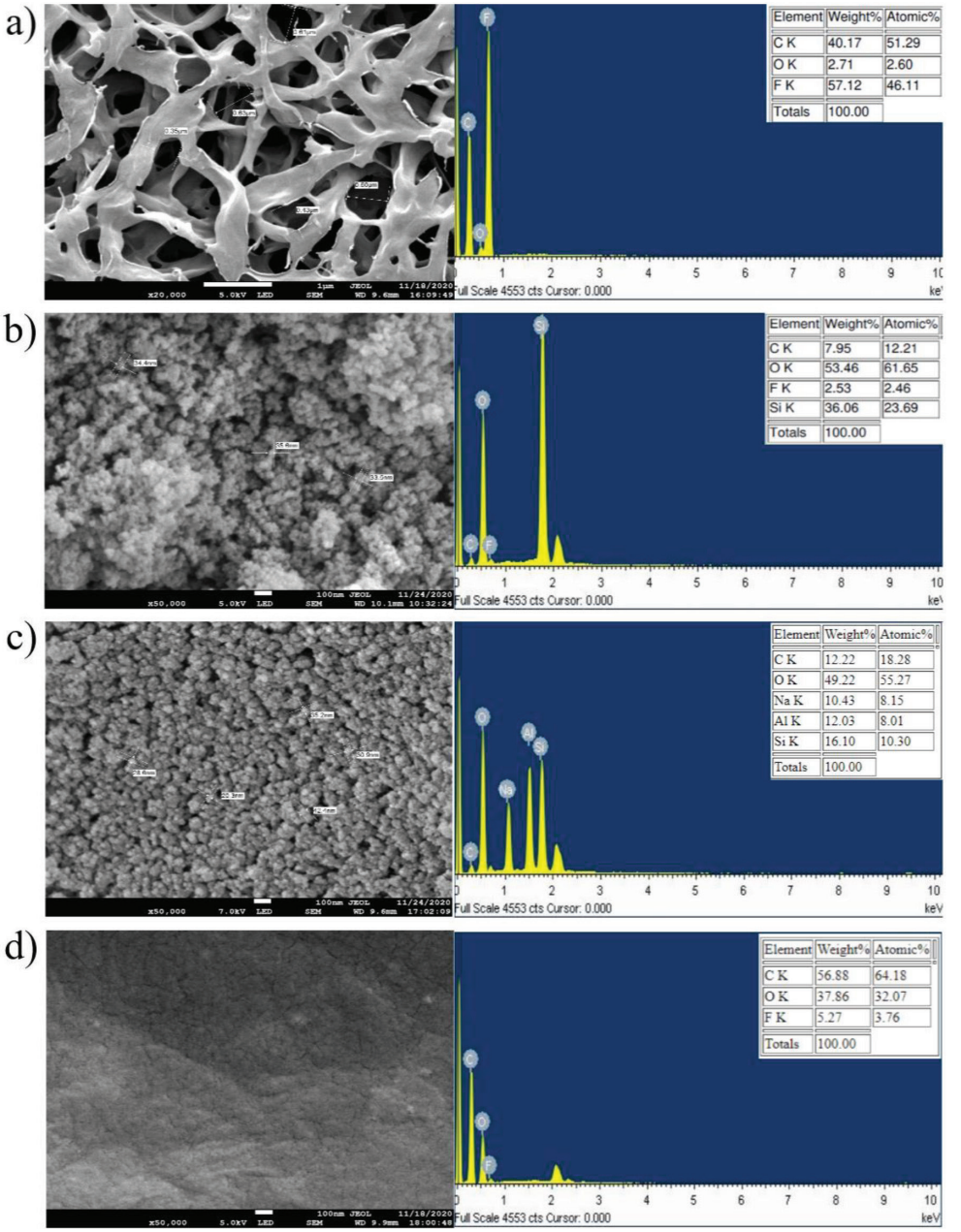

Figure 4: FESEM EDX of (a) pristine PVDF membrane at 20,000x magnification, (b) PVDF + 0.1% nanosilica at 50,000x magnification, (c) PVDF + 0.1% nanozeolite at 50,000x magnification, (d) PVDF + 0.1% GO at 50,000x magnification

Based on the results of ICP-MS analysis, a significant amount of 1,212 ppm Ti was detected in the unexposed nylon samples compared to 1,326 ppm Ti after exposure (Table 2). Although the amount of Ti measured was relatively high, it cannot be used to represent the actual amount of Ti filtered from the nylon filters used in the NRD. Due to the substantial presence of Ti

Table 1: Chemical composition obtained by EDX analysis

	Weight (%) of Elements (Wt%)					
Sample (w/v)	**Carbon (C)**	**Oxygen (O)**	**Fluorine (F)**	**Silica (Si)**	**Aluminium (Al)**	**Sodium (Na)**
Pristine PVDF	40.17	2.71	57.12	-	-	-
Nanosilica 0.1%	8.79	53.20	4.08	33.93	-	-
Nanosilica 0.5%	7.88	54.17	-	37.95	-	-
Nanosilica 1%	7.89	51.83	-	40.28	-	-
Nanozeolite 0.1%	9.37	44.95	4.59	17.03	13.29	10.77
Nanozeolite 0.5%	9.05	38.90	-	23.70	17.43	10.92
Nanozeolite 1%	5.71	27.79	-	34.03	22.70	9.76
GO 0.1%	55.87	40.67	3.46	-	-	-
GO 0.5%	57.12	41.90	0.98	-	-	-
GO 1%	60.07	39.93	0.00	-	-	-

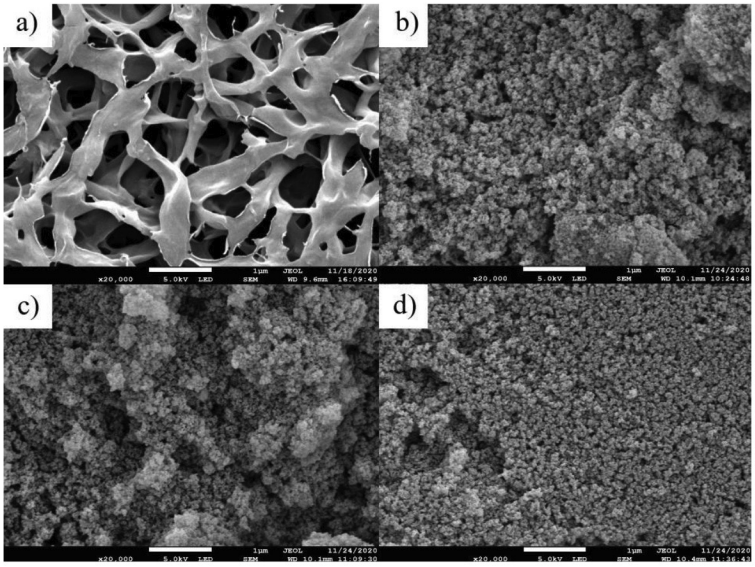

Figure 5: FESEM of PVDF membrane deposited with (a) no additional nanomaterials, (b) 0.1% w/v nanosilica, (c) 0.5% w/v nanosilica, (d) 1.0% w/v of nanosilica at 20,000x magnification

element in the unexposed nylon membrane, the usage of nylon membrane in the NRD is strictly unsuitable for TiO_2 nanoparticles sampling and invalid for Ti element analysis. Besides, each nylon filter has a different amount of Ti without being disclaimed in the nylon information data sheet. Similar results were recorded in previous studies by (Cena *et al*., 2011) and Mines *et al*. (2016), suggesting that TiO_2 was used in the bleaching process of the nylon filter. The presence of Ti from the original filter would interfere with the accuracy of the evaluation of Ti captured from air contaminated with TiO_2. Importantly, all newly developed nanofilters and the pristine PVDF membrane did not show Ti background levels. As shown in Table 2, the nanozeolite filter (0.1% w/v) showed the highest concentration of Ti captured (81.7 ppm)

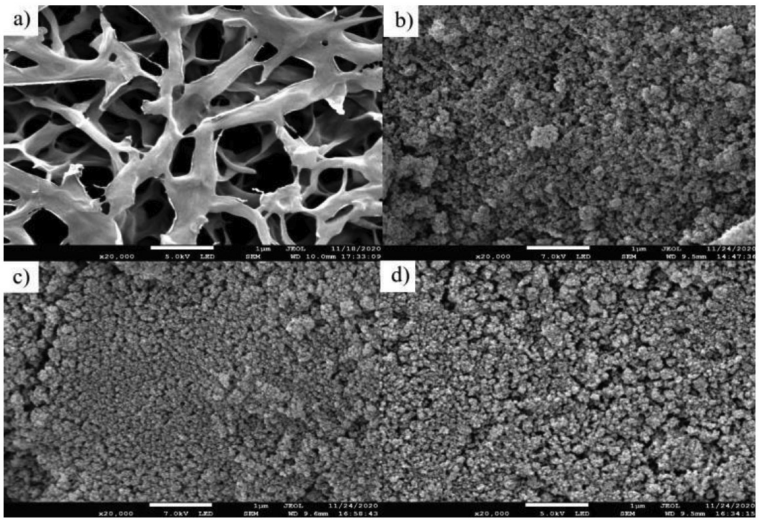

Figure 6: FESEM of PVDF membrane deposited with (a) no additional nanomaterials, (b) 0.1% w/v nanozeolite, (c) 0.5% w/v nanozeolite, (d) 1.0% w/v of nanozeolite at 20,000x magnification

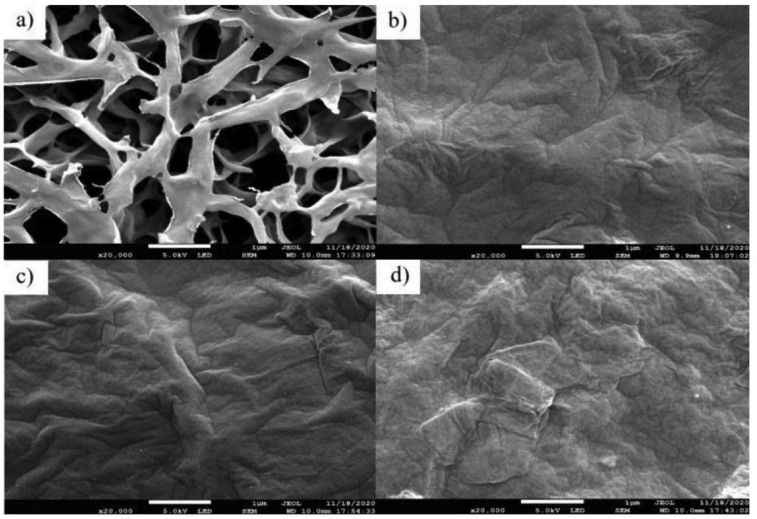

Figure 7: FESEM of PVDF membrane deposited with (a) no additional nanomaterials, (b) 0.1% w/v GO, (c) 0.5% w/v GO, (d) 1.0% w/v of GO at 20,000x magnification

compared to other materials such as nanosilica (56.7 ppm) and graphene oxide (8.2 ppm) filters.

Nanozeolite is a nano-size hydrated porous crystalline aluminosilicate with open framework structures of tetrahedral SiO_4^{4-} and AlO_4^{3-} units (Ng *et al*., 2015). It also has an open three-dimensional structure with pores and empty spaces in the molecular dimension allowing for potential chemical molecule adsorption. The chemical bond between zeolite and Ti has been demonstrated by several previous studies where bonds such as Ti-O-Na can occur. Liu *et al.* (1992) initially incorporated TiO_2 into zeolite Y cavities through the ion exchange. Following this, much research has been done on TiO_2/nanozeolite as a photocatalyst in many chemical reactions, further suggesting a stable interaction between both compounds. To our

Table 2: Ti element concentrations from various types of filters quantified using ICPMS

Filters	Ti Concentration (mg kg^{-1})
PVDF (non-exposed)	Not detected
Nylon (non-exposed)	1212 ± 33.5
PVDF (exposed)	Not detected
Nylon (exposed)	1326.75 ± 28.25
PVDF + NS 0.01%	Not detected
PVDF + NS 0.05%	17.4 ± 0.6
PVDF + NS 0.1%	56.7 ± 1.5
PVDF + NS 0.5%	28.0 ± 1.0
PVDF + NS 1.0%	8.2 ± 0.4
PVDF + NZ 0.01%	14.1 ± 0.3
PVDF + NZ 0.05%	Not detected
PVDF + NZ 0.1%	81.7 ± 3.4
PVDF + NZ 0.5%	34.7 ± 1.7
PVDF + NZ 1.0%	28.4 ± 0.4
PVDF + GO 0.01%	Not detected
PVDF + GO 0.05%	Not detected
PVDF + GO 0.1%	6.0 ± 0.2
PVDF + GO 0.5%	8.2 ± 0.4
PVDF + GO 1.0%	Not detected

knowledge, this is the first time that nanozeolite was identified to capture Ti nanoparticles in the air.

Like nanozeolite, nanosilica also showed good interaction with TiO_2. Nanosilica possesses a great adsorptive material to many inorganic materials due to its promising properties such as having a large surface area and porous structure (Mironyuk *et al*., 2019; Zhang *et al*., 2020). The use of nanosilica as a filter to trap TiO_2 from the air has not been studied. Ti that a nanosilica PVDF filter has successfully trapped is most likely chemically bound through chemical bonds with other elements present in the filter such as Ti-O-Ti, Ti-O-H and Ti-O-Si. The chemical bond between Si and Ti has been reported in previous studies (Rasalingam *et al*., 2013; Dalod *et al*., 2017; Hakki *et al*., 2017; Parimalam *et al*., 2019). However, such studies did not use silica to trap Ti from the air. It can be suggested that chemical bonds between Ti and Si can be attributed to this study. Dipole attraction between the negative charge from nanosilica and the positive charge from Ti can also cause the absorption process to occur during filtration. Physical attraction by dipole-dipole forces between negatively charged SiO_2 and positively charged TiO_2 may also likely aid in the adsorption during the filtration process (Gibson, 2014).

TiO_2 nanomaterials can still be trapped by PVDF-GO membranes even though the amount is insignificant. The capturing efficiency exhibited by the PVDF-GO membrane is somewhat less than that of nanosilica and nanozeolite filters, possibly due to the limited cavities observed on the GO membrane. Thus, this may affect the membrane's efficiency particularly for capturing the TiO_2 nanoparticles due to the flat surface and the lack of cavity pores.

Conclusion

After going through important phases in this study, the processes of producing basic materials into nanomaterials have been successfully produced from agricultural waste (rice husk) which is generally known to be cheap, easy to obtain and have high environmental sustainability. Due to its outstanding performance in chemical adsorption, graphite in the form of graphene oxide was also used to produce nanofilter in this work. Results obtained from this work showed that all the nanomaterials were successfully deposited on the PVDF membrane and able to capture TiO_2 nanoparticles with nanozeolite showing the best result compared to nanosilica and GO. Although a certain amount of Ti element was detected using ICPMS when exposing the nylon membrane to the TiO_2 nanoparticles, it should be noted that the unexposed nylon membrane contained high background levels of Ti, thus, rendering them unsuitable to be used for TiO_2 nanoparticles air sampling. Therefore, it can be suggested that nanozeolite from RHA can be a good source of nanomaterials to produce nanofilter to capture TiO_2 nanoparticles using the NRD system.

Acknowledgements

This research study were supported financially by National Institute of Occupational Safety and Health (NIOSH) Malaysia (Ref. No:NIOSH/NP.SH.19/2019-CRD) and UiTM Supervision Initiatives Grant (Ref. No: PY/2022/01853).

References

Arahman, N., Mulyati, S., Fahrina, A., Muchtar, S., Yusuf, M., Takagi, R., Matsuyama, H., Nordin, N. A. H., & Bilad, M. R. (2019). Improving water permeability of hydrophilic PVDF membrane prepared via blending with organic and inorganic additives for humic acid separation. *Molecules*, *24*(22), 4099.

Artkla, S., Kim, W., Choi, W., & Wittayakun, J. (2009). Highly enhanced photocatalytic degradation of tetramethylammonium on the hybrid catalyst of titania and MCM-41 obtained from rice husk silica. *Applied Catalysis B: Environmental*, *91*(1-2), 157-164. https://doi.org/10.1016/j.apcatb.2009.05.019

Cena, L. G., Anthony, T. R., & Peters, T. M. (2011). A personal nanoparticle respiratory deposition (NRD) sampler. *Environmental Science and Technology*, *45*(15), 6483-6490. https://doi.org/10.1021/es201379a

Chun, J., & Lee, J. H. (2020). Recent progress on the development of engineered silica particles derived from rice husk. *Sustainability (Switzerland*, *12*(24), 1-19. https://doi.org/10.3390/su122410683

Dalod, A. R. M., Henriksen, L., Grande, T., & Einarsrud, M.-A. (2017). Functionalized TiO_2 nanoparticles by single-step hydrothermal synthesis: The role of the silane coupling agents. *Beilstein Journal of Nanotechnology*, *8*(1), 304-312.

Dréno, B., Alexis, A., Chuberre, B., & Marinovich, M. (2019). Safety of titanium dioxide nanoparticles in cosmetics. *Journal of the European Academy of Dermatology and Venereology*, *33*, 34-46.

Edu, O., & Lai, E. P. C. (2015). Airborne silica and titanium dioxide nanoparticles: Collection with Aqueous surfactant or chemical reagent. *Journal Nanomaterials & Molecular Nanotechnology*, *4*(3), 2-6.

Fichera, O., Alpan, L., Laloy, J., Tabarrant, T., Uhrner, U., Ye, Q., Mejia, J., Dogné, J.-M., & Lucas, S. (2019). Characterization of water-based paints containing titanium dioxide or carbon black as manufactured nanomaterials before and after atomization. *Applied Nanoscience*, *9*(4), 515-528.

Ghasemi, Z., & Younesi, H. (2012). Preparation of free-template Nanometer-Sized Na-A and -X Zeolites from rice husk ash. *Waste and Biomass Valorization*, *3*, 61-74. https://doi.org/10.1007/s12649-011-9084-4

Gibson, L. T. (2014). Mesosilica materials and organic pollutant adsorption: Part

A removal from air. *Chemical Society Reviews*, *43*(15), 5163-5172. https://doi.org/10.1039/c3cs60096c

Hakki, A., Yang, L., Wang, F., & Macphee, D. E. (2017). The effect of interfacial chemical bonding in TiO_2-SiO_2 composites on their photocatalytic NOx abatement performance. *JoVE (Journal of Visualized Experiments)*, *125*, e56070.

Horváth, T., Papp, A., Kiricsi, M., Igaz, N., Trenka, V., Kozma, G., Tiszlavicz, L., Rázga, Z., & Vezér, T. (2019). Investigation of the effect of titanium dioxide nanorods on the lungs in a subacute rat model. *Orvosi Hetilap*, *160*(2), 57-66.

Hossain, S. S., Mathur, L., & Roy, P. K. (2018). Rice husk/rice husk ash as an alternative source of silica in ceramics: A review. *Journal of Asian Ceramic Societies*, *6*(4), 299-313. https://doi.org/10.1080/21870764.2018.1539210

Hou, Y., Lv, S., Liu, L., & Liu, X. (2020). High-quality preparation of graphene oxide via the Hummers' method: Understanding the roles of the intercalator, oxidant, and graphite particle size. *Ceramics International*, *46*(2), 2392-2402.

Inagaki, I., Takechi, T., Shirai, Y., & Ariyasu, N. (2014). Application and features of titanium for the aerospace industry. *Nippon Steel & Sumitomo Metal Technical Report*, *106*(106), 22-27.

Jeevanandam J, Barhoum A, Chan YS, Dufresne A, D. M. (2018). Review on nanoparticles and nanostructured materials: History, sources, toxicity and regulations. *Beilstein Journal of Nanotechnology*, 1050-1074.

Khan, I., Saeed, K., & Khan, I. (2019). Nanoparticles: Properties, applications and toxicities. *Arabian Journal of Chemistry*, *12*(7), 908-931. https://doi.org/10.1016/j.arabjc.2017.05.011

Koehler, K. A., & Peters, T. M. (2015). New Methods for Personal Exposure Monitoring for Airborne Particles. *Current Environmental Health Reports*, *2*(4), 399-411. https://doi.org/10.1007/s40572-015-0070-z

Kumagai, S., & Sasaki, J. (2009). Carbon/silica composite fabricated from rice husk by means of binderless hot-pressing. *Bioresource Technology*, *100*(13), 3308-3315. https://doi.org/10.1016/j.biortech.2009.02.001

Liu, X., Iu, K.-K., & Thomas, J. K. (1992). Encapsulation of TiO_2 in zeolite Y. *Chemical Physics Letters*, *195*(2-3), 163-168.

Mines, L. W. D., Park, J. H., Mudunkotuwa, I. A., Anthony, T. R., Grassian, V. H., & Peters, T. M. (2016). Porous polyurethane foam for use as a particle collection substrate in a nanoparticle respiratory deposition sampler. *Aerosol Science and Technology*, *50*(5), 497-506. https://doi.org/10.1080/02786826.2016.1164828

Mironyuk, I. F., Gun'ko, V. M., Vasylyeva, H. V, Goncharuk, O. V, Tatarchuk, T. R., Mandzyuk, V. I., Bezruka, N. A., & Dmytrotsa, T. V. (2019). Effects of enhanced clusterization of water at a surface of partially silylated nanosilica on adsorption of cations and anions from aqueous media. *Microporous and Mesoporous Materials*, *277*, 95-104.

Musial, J., Krakowiak, R., Mlynarczyk, D. T., Goslinski, T., & Stanisz, B. J. (2020). Titanium dioxide nanoparticles in food and personal care products—what do we know about their safety? *Nanomaterials*, *10*(6), 1110.

Nassrullah, H., Makanjuola, O., Janajreh, I., AlMarzooqi, F. A., & Hashaikeh, R. (2020). Incorporation of nanosized LTL zeolites in dual-layered PVDF-HFP/cellulose membrane for enhanced membrane distillation performance. *Journal of Membrane Science*, *611*, 118298. https://doi.org/https://doi.org/10.1016/j.memsci.2020.118298

Ng, E., Awala, H., Tan, K., Adam, F., Retoux, R., & Mintova, S. (2015). EMT-type zeolite nanocrystals synthesized from rice husk. *Microporous and Mesoporous Materials*, *204*, 204-209. https://doi.org/10.1016/j.micromeso.2014.11.017

Papp, A., Horváth, T., Igaz, N., Gopisetty, M. K., Kiricsi, M., Berkesi, D. S., Kozma, G., Kónya, Z., Wilhelm, I., & Patai, R. (2020). Presence of titanium and toxic effects observed in rat lungs, kidneys, and central nervous system in vivo and in cultured astrocytes in vitro on exposure by titanium dioxide nanorods. *International Journal of Nanomedicine*, *15*, 9939.

Parimalam, M., Islam, M. R., & Yunus, R. M. (2019). Effects of nanosilica and titanium oxide on the performance of epoxy-amine nanocoatings. *Journal of Applied Polymer Science*, *136*(35), 47901.

Park, J. H., Mudunkotuwa, I. A., Mines, L. W. D., Anthony, T. R., Grassian, V. H., & Peters, T. M. (2015). A granular bed for use in a nanoparticle respiratory deposition sampler. *Aerosol Science and Technology*, *49*(3), 179-187. https://doi.org/10.1080/02786826.2015.1013521

Patil, R., Dongre, R., & Meshram, J. (2014). Preparation of silica powder from rice husk. *Journal of Applied Chemistry (IOSR-JAC), 27*, 26-29.

Pham, T. D., Bui, T. T., Nguyen, V. T., Bui, T. K. Van, Tran, T. T., Phan, Q. C., Pham, T. D., & Hoang, T. H. (2018). Adsorption of polyelectrolyte onto nanosilica synthesized from rice husk: Characteristics, mechanisms, and application for antibiotic removal. *Polymers*, *10*(2), 220.

Premaratne, W. A. P. J., Priyadarshana, W. M. G. I., Gunawardena, S. H. P., & De Alwis, A. A. P. (2014). Synthesis of nanosilica from paddy husk ash and their surface functionalization. *Journal of Science of the University of Kelaniya Sri Lanka*, *8*(2013), 33-48. https://doi.org/10.4038/josuk.v8i0.7238

Rafiee, E., Shahebrahimi, S., Feyzi, M., & Shaterzadeh, M. (2012). Optimization of synthesis and characterization of nanosilica produced from rice husk (a common waste material. *International Nano Letters*, *2*(1), 1-8. https://doi.org/10.1186/2228-

Ramos-Galicia, L., Mendez, L. N., Martínez-Hernández, A. L., Espindola-Gonzalez, A., Galindo-Esquivel, I. R., Fuentes-Ramirez, R., & Velasco-Santos, C. (2013). Improved performance of an epoxy matrix as a result of combining graphene oxide and reduced graphene. *International Journal of Polymer Science*, *2013*, 1-7.

Rasalingam, S., Kibombo, H. S., Wu, C.-M., Budhi, S., Peng, R., Baltrusaitis, J., & Koodali, R. T. (2013). Influence of Ti-O-Si hetero-linkages in the photocatalytic degradation of Rhodamine B. *Catalysis Communications*, *31*, 66-70.

Ruan, W.-X., Liao, J., Wang, G.-Q., Zhang, X.-W., Wang, J., & Ji, J.-B. (2015). Hydrophilic modification of polyvinylidene fluoride (PVDF) membrane with ionic liquid grafted Nano-SiO_2 particles. *Gao Xiao Hua Xue Gong Cheng Xue Bao/Journal of Chemical Engineering of Chinese Universities*, *29*, 185-194. https://doi.org/10.3969/j.issn.1003-9015.2015.01.028

Ruey Ong, H., Mohd Eqhwan Iskandar, W., Khan, M. R., & Md. (2020). Rice Husk Nanosilica Preparation and Its Potential Application as Nanofluids. In *Engineered Nanomaterials - Health and Safety.* IntechOpen. https://doi.org/10.5772/intechopen.89904

Scorrano, S., Mergola, L., Bello, M., Lazzoi, M., Vasapollo, G., & Del Sole, R. (2015). Molecularly imprinted composite membranes for selective detection of 2-deoxyadenosine in urine samples. *International Journal of Molecular Sciences*, *16*, 13746-13759. https://doi.org/10.3390/ijms160613746

Skocaj, M., Filipic, M., Petkovic, J., & Novak, S. (2011). Titanium dioxide in our everyday life; Is it safe? *Radiology and Oncology*,

45(4), 227-247. https://doi.org/10.2478/v10019-011-0037-0

Titanium Dioxide: OSH Answers. (2017). https://www.ccohs.ca/oshanswers/chemicals/chem_profiles/titanium_dioxide.html

Ursini, C. L., Cavallo, D., Fresegna, A. M., Ciervo, A., Maiello, R., Tassone, P., Buresti, G., Casciardi, S., & Iavicoli, S. (2014). Evaluation of cytotoxic, genotoxic and inflammatory response in human alveolar and bronchial epithelial cells exposed to titanium dioxide nanoparticles. *Journal of Applied Toxicology*, *34*(11), 1209-1219.

Vaquero, C., Gutierrez-Ca~nas, C., Galarza, N., & Ipi~na, J. L. L. De. (2016). Exposure assessment to engineered nanoparticles handled in industrial workplaces: The case of alloying nano-TiO_2 in new steel formulations. *Journal of Aerosol Science*, *102*, 1-15.

Victor, F. S., Kugarajah, V., Bangaru, M., Ranjan S., & Dharmalingan S. (2021). Electrospun nanofibers of polyvinylidene fluoride incorporated with titanium nanotubes for purifying air with bacterial contamination. *Environmental Science and Pollution Research, 28*, 37520-37533.

Wang, Z., Zhang, W., Yu, J., Zhang, L., Liu, L., Zhou, X., Huang, C., & Fan, Y. (2019). Preparation of nanocellulose/filter paper (NC/FP) composite membranes for high-performance filtration. *Cellulose*, *26*(2), 1183-1194. https://doi.org/10.1007/s10570-018-2121-8

Yuvakkumar, R., Elango, V., Rajendran, V., & Kannan, N. (2014). High-purity nano silica powder from rice husk using a simple chemical method. *Journal of Experimental Nanoscience*, *9*(3), 272-281. https://doi.org/10.1080/17458080.2012.656709

Zhang, J., Zhai, J., Zheng, H., Li, X., Wang, Y., Li, X., & Xing, B. (2020). Adsorption, desorption and coadsorption behaviors of sulfamerazine, Pb (II) and benzoic acid on carbon nanotubes and nano-silica. *Science of the Total Environment*, *738*, 139685.

Zhou, Z. F., Huang, H., & Liu, N. C. (2001). Kinetics and mechanism of grafting of oleic acid onto acrylonitrile-butadiene-styrene terpolymer. *European Polymer Journal*, *37*(10), 1967-1974. https://doi.org/10.1016/S0014-3057(01)00080-5